INFERIOR ALVEOLAR NERVE TRANSPOSITION– AN IN VITRO COMPARISON BETWEEN PIEZOSURGERY AND CONVENTIONAL BUR USE

Marc C. Metzger, MD, DDS
K. H. Bormann, DDS
R. Schoen, MD, DDS
N. C. Gellrich, MD, DDS
R. Schmelzeisen, MD, DDS

KEY WORDS

Piezoelectric
Bur
Inferior alveolar nerve
Bone

Marc C. Metzger, MD, DDS, *is a resident,* ***R. Schoen, MD, DDS,*** *is an assistant professor, and* ***R. Schmelzeisen, MD, DDS,*** *is chairman professor in the Department of Oral and Maxillofacial Surgery, University Hospital Freiburg, Albert Ludwigs University Freiburg, Freiburg, Germany. Address correspondence to Dr Metzger at Department of Oral and Maxillofacial Surgery, University Freiburg, Hugstetter Strasse 55, D-79106 Freiburg, Germany (e-mail: Marc_Metzger@gmx.net).*

K. H. Bormann, DDS, *is a resident and* ***N. C. Gellrich, MD, DDS,*** *is chairman professor in the Department of Oral and Maxillofacial Surgery, University Hospital Hannover, Medical University, Hannover, Germany.*

An in vitro comparison between a new ultrasound-based piezoelectric device and a conventional bur was performed for lateralization or transposition of the inferior alveolar nerve to evaluate the effects on soft and hard tissue. Transposition of the inferior alveolar nerve was performed in the cadaver mandibles of 10 sheep: the left nerve was uncovered with a saline-cooled diamond-coated spherical bur (2000 rpm), and the right nerve was uncovered with the piezoelectric device mounted with a spherical diamond tip. The surface, the zone of bone defect, and the nerve were examined by light microscopy and laser microscopy. Bone treated with the rotary bur showed significantly smoother surfaces and shallower defect zones (50 μm) in comparison with the piezoelectric device (150 μm). Lesions of the epineurium and an increased amount of bone particles were found in the lesions prepared with the piezoelectric device. In vitro preparation with the piezoelectric device was more invasive to the bone than was a conventional diamond bur. Touching the inferior alveolar nerve resulted in roughening of the epineurium without affecting deeper structures. The degree of injury was lower than when using the conventional rotary bur.

INTRODUCTION

Dental implant placement in the severely atrophic posterior mandible can be compromised by an inadequate vertical volume of bone above the neurovascular bundle. Although lateralization of the inferior alveolar nerve (IAN) is often performed as an alternative to augmentation techniques, there is a risk of nerve injury through primary surgical trauma or secondary complications such as edema or hematoma. In spite of possible surgical reconstruction of nerves, efforts have been made to minimize these disadvantages.[1–3] Initially, a corticotomy that includes the mental foramen is performed, then the remaining cancellous lamella covering the IAN is

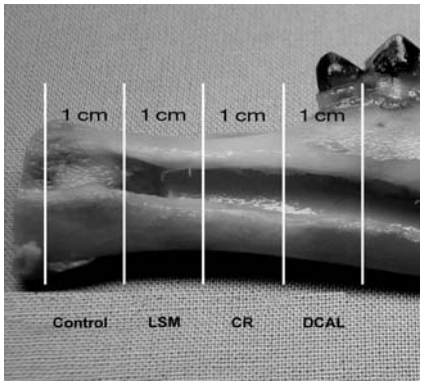

FIGURE 1. Four cross sections of cadaver sheep mandibles were performed. From left to right: control, laser surface measurement, cracks, decalcification.

removed.[4,5] To protect the nerve, a thin bent spatula inserted through the mental foramen is placed between the neurovascular bundle and the cancellous lamella. The IAN is retracted from the mandibular canal, the implants are inserted, and the nerve is positioned lateral to the implants. The anterior incisive branch is not affected. Transposition of the IAN requires a corticotomy including the mental foramen. After transection of the anterior incisive branch the nerve is transposed posteriorly.[4,6,7] Despite extreme caution and measures, injuries caused by compression or direct trauma by the rotating instrument cannot be excluded. A reduction in IAN lesions has been reported with the use of ultrasonic devices.[8] New cutting devices using piezoelectricity possess a high oscillating frequency of over 20 000 cycles per second and an oscillating motion of 20 to 200 μm; when touching mineralized hard tissue, they work like a pneumatic hammer, and small particles of bone are shattered to form microcracks and debris.[9,10] Such an effect does not occur in soft tissue because of its elasticity. In contrast to conventional ultrasonic cutting devices, the piezoelectric device is 3 times more powerful and has a modified oscillating movement. This results in an improved bone cut and decreased heat development.[8,11,12]

The aim of this study is to compare the effects of piezoelectric and conventional drilling instruments on the IAN and the adjacent bone in cadaver sheep mandibular specimens after transposition of the IAN.

MATERIALS AND METHODS

Ten sheep mandibles were dissected from the surrounding soft tissue and the periostium without harming the mental and mandibular nerves. On the left side, the canal was opened with a diamond-coated spherical drill under constant irrigation with saline solution. The IAN was protected by a thin bent spatula inserted in the mental foramen.[13] Preparation of the right side was carried out with the piezoelectric device (Mectron Piezosurgery Device, Mectron, Genova, Italy) mounted with a diamond-coated spherical tip. The device consisted of a piezoelectric hand piece and a regulation panel. Functional frequencies of 25 to 29 kHz and digital modulation in "boosted" mode with 30 kHz were selected. A jet of physiological saline solution provided constant cooling. The highest power mode boosted was selected.[14]

Bone

The bone areas of interest were cross sectioned with a circular saw (Figure 1). The first cut was placed at the level of the mental foramen. The anterior section served as a control for the surface measurement. The genuine inferior alveolar canal showed a similar cross section to the manipulated area. The samples were fixed in 3.5% formaldehyde (Figure 1).

Laser surface measurements

Surface measurements were carried out with a laser surface measurement (LSM) system (UBM, Messtechnik GmbH, Ettlingen, Germany).[15] To compare the surface structure produced by both preparation methods, the 10 bone sections of each group were cut longitudinally at the anterior side of the mandibular canal, providing a horizontal surface necessary for the laser measurements in an area of 2.0×0.5 mm. The values shown in Table 1 were measured on all 40 bone pieces.

Detection of microcracks

The samples were dehydrated with ascending alcohol concentrations. For the detection of microcracks, the samples were stained en bloc with 1% basic fuchsin (basic fuchsin, Merck 15937, Darmstadt, Germany).[16–18] The samples were then embedded in Technovit (Technovit 7200 VLC, Heraeus Kulzer, Wehrtheim, Germany). After 12 hours curing under ultraviolet light, 250-μm thick sections were cut

TABLE 1
Values of the laser surface measurements

Abbreviation	Explanation
Ra	The most widely used description of a surface. It is a mean line at the level in which all valleys can be filled by all peaks. The arithmetic mean of the deviations up and down from this theoretical mean line is Ra.
Rmax	The maximum peak-to-valley height of the profile.
Rt	The distance from the highest peak to the deepest valley.

(Microslice 2, Metals Research, Cambridge, UK). These were mounted (Cyanacrylat, Loctite, München, Germany) onto acrylicglass ($50 \times 50 \times 3$ mm^3, 05370, Mertin, Freiburg, Germany) and ground to a thickness of 100 μm.

The initial investigation was performed at ×100 and ×200 magnification under a fluorescent light microscope (Axio Cam 2 Plus, Zeiss, Germany). Microcracks appeared orange under green light ($\lambda = 546$). To obtain quantitative data from the defect zone, the broadest part was observed at the lower magnification. Measurements were evaluated with ImageJ V1.3 (Java Applet, freeware; Sun Microsystems, Inc, Santa Clara, Calif) in a blinded format. The thicknesses of the defects were determined with the plumb bob.

Decalcification

The samples were submerged in 50% formic acid for 1 week and dehydrated with ascending alcohol concentrations for 12 hours. Finally, the samples were embedded in paraffin, sectioned (8 μm), and stained (hematoxylin and eosin [H&E] and Elastica van Giesson [EVG]).

Analysis of the IAN

After exposure, the IAN was carefully removed from the canal starting at the mental foramen. A circular stitch (Vicryl, 5-0, Ethilon, Lenneke Marelaan, Belgium) was inserted for further identification of the prepared lateral side. The nerve was then mobilized between the mental foramen and the first molar. A second stitch was placed at the level of the first molar. The IAN was sectioned and removed posteriorly from these marks. The pieces of nerve were submerged in 3.5% formaldehyde for 1 week. India ink staining was carried out to mark the anterior side of the nerve, allowing spatial orientation after cutting.

The nerves were cut perpendicular to the fascicles within the anterior section and lengthwise within the posterior section. All samples were then dehydrated with ascending alcohol concentrations, embedded in paraffin, sectioned (8 μm), and stained (H&E, EVG, Goldner 1). Evaluation of the nerve cross sections was performed with a microscope (Axio Cam 2 Plus) at ×25 and ×100 magnification.

TABLE 2

Surface structure parameters of natural bone and of bone dissected with rotary bur and piezoelectric device (μm)

	Natural Bone	Rotary Bur	Piezoelectric Device
Ra	2.93	1.94	2.61
Rmax	33.51	18.80	27.26
Rt	35.52	19.62	28.60

RESULTS

Bone

Laser Surface Measurements

The results of the topographic measurements of original bone, bone dissected with the rotary bur, and bone dissected with the piezoelectric device are shown in Table 2. Figure 2A through C shows the 3-dimensional reconstructions of measurement points (LSM). The resolution of measurements was 1000 points/1 mm to 500 points/0.5 mm. Figure 3A through C demonstrates the histological photomicrographs of bone fragments (decalcification).

One-way analysis of variance (SPSS version 9.0) showed significant differences among the values for all groups ($P_{RA} = .046$; $P_{Rmax} = .020$; $P_{Rt} = .014$).

Detection of Microcracks

The rotary bur produced a smooth cut bone edge. No separation of the bone lamella occurred (Figure 4A and B). The defect zone of the samples prepared with the piezoelectric device had an average depth of approximately 170 μm (Table 3). The defect zone created with the rotary instrument had an average depth of approximately 54 μm.

The piezoelectric device produced an irregular surface. The structure of the bone worked loose, comparable with a brittle mineral (Figure 4C and D). Application of the Student *t* test for independent samples (SPSS version 9.0) revealed a significant difference between the 2 groups ($F = 7.252$, thus no equal variances; $P = .000$).

Findings at the IAN

The selected localization allowed mobilization and removal of the nerve section. The India ink marks at the anterior epineurium could be easily identified in all samples.

The vessels were always visible on the anterior half of the crosswise-cut nerves (Figure 5B and E). All sections of nerve exhibited a polyfascicular structure. Because the section was anterior, the nerve demonstrated fewer fascicles and more fat cells in the internal epineurium.[19]

The external epineurium showed longitudinal collagen fibers.[20] The perineurium consisted of perineural epithelium with predominantly longitudinal collagen fibrils and fibrocytes between them.

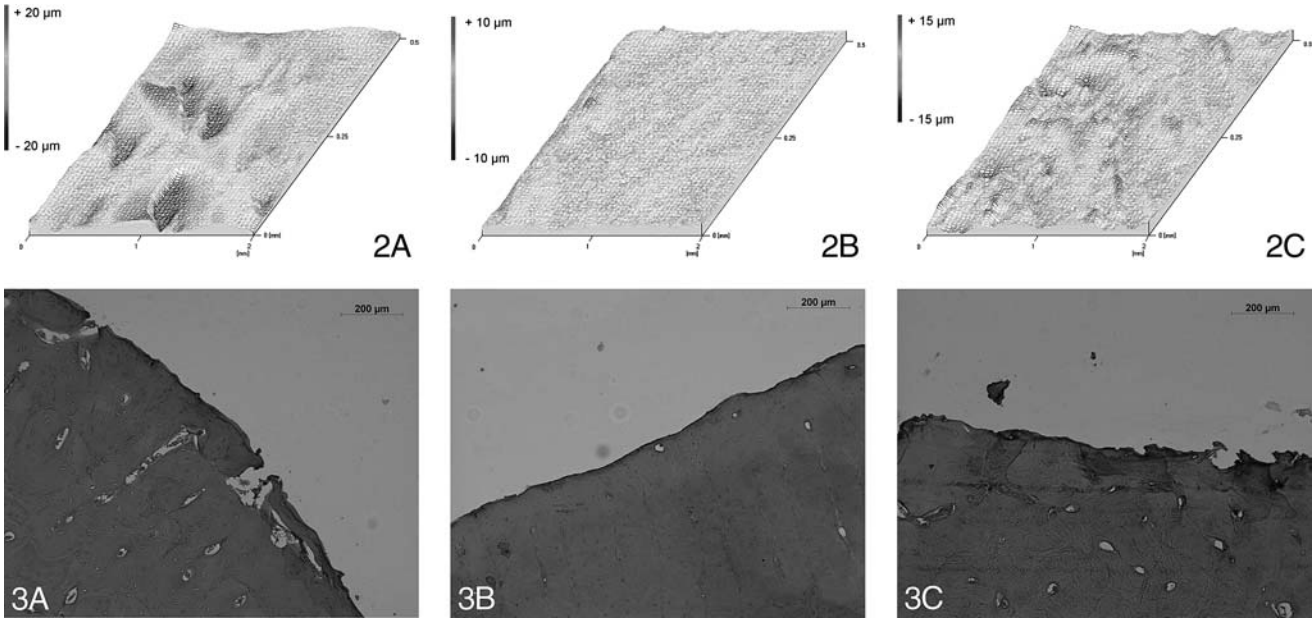

FIGURES 2 and 3. FIGURE 2. UBM images of calculated, polynomially transformed surface. (A) Surface of original bone. (B) Bone surface after preparation with the rotary bur. (C) Bone surface after preparation with the piezoelectric device. FIGURE 3. Histological photomicrographs demonstrating the surface of bone fragments (decalcification group) (hematoxylin and eosin, magnification ×100). (A) Edge of original bone. (B) Edge of bone cut with rotary bur. (C) Edge of bone cut with piezoelectric device.

The histological pictures of both groups displayed typical characteristics of the different methods of preparation. No lesions could be observed, and isolated bone particles were found at the epineurium in the group prepared with the rotary bur (Figure 5A through C). With the piezoelectric device, the epineurium had a rough appearance. Bone particles were found in and on the epineurium (Figure 5D through F).

Other parts of the nerves lying within the epineurium were not affected either by the piezoelectric device or the rotary bur. The extension of the irritation zone, noticed in lengthwise sections (Figure 5D), was visible in all areas touched by the piezoelectric device.

DISCUSSION

Difficulties with implant insertion arise in cases of atrophic jaws. The limiting factor in such cases is the anatomical course of the IAN. For lateralization or transposition of the nerve, the 2- to 4-mm cortical bone, the thin cancellous bone, and a fibrous sheath (paraneurium) have to be removed. In addition, 64% of patients demonstrate a cortical lamella within the cancellous lamella.[21]

A rotary bur is reported to cut faster and produce a deeper cut than a piezoelectric device.[22,23] The cutting efficiency of a piezoelectric device depends on the adjustment of the instrument tip, with the highest efficiency when the tip is kept flat.[24] The best angle resulting in a higher cutting rate is reported to be between 0° and 10° of the orthogonal preparation axis.[22] In comparison, the efficiency of the rotary bur was independent of the adjustments.

In the presented study, it was observed macroscopically that the irrigation liquid rinsed the bone particles into the nerve canal during preparation and exposure of the nerve in both techniques. This was also observed microscopically with a higher particle density on the epineurium after the use of the piezoelectric device. In contrast, the rotating motion of the rotary bur carried splinters away from the area of surgery.

The rotary bur produced regular bone edges, whereas the piezoelectric device produced loosened bone edges. The average surface roughness (Rmax) was significantly higher for the samples prepared with the piezoelectric device (27.26 µm) than for those prepared with the rotary bur (18.80 µm). Similar results have been shown previously.[23,25]

Faster initial wound healing and a consequent reduction in infection risk after preparation with ultrasonic instruments have been observed in vivo in animals.[25,26] The improved healing tendency could be because of the pronounced bone edge roughness, which would allow a

greater number of osteoclasts and osteoblasts to act simultaneously. This effect was observed with defects reaching into the cancellous bone.[25] Remaining within the cortex, a rough surface reduced the regeneration process. Beginning at the periostium, a smooth surface produced with a rotary bur seemed to be more conductive to regeneration.[23] However, there was no significant difference in wound healing after 42 to 90 days in both studies.[25,27]

The formation of microcracks in dentin by the swinging ultrasonic tip has already been observed in root-end preparations.[9] According to Burr and Stafford,[28] criteria for the identification of microcracks in bone are (1) an intermediate size ranging between the smaller canaliculi and the larger vascular channels (average size of the microcracks produced by stress fractures; eg, in the human rib, it is approximately 90 μm[18]), (2) sharp borders with a basic fuchsin area around them, (3) staining throughout the entire depth, and (4) corners of the microcracks that appear more deeply stained than the intervening space. The computation of form and volume is problematic because the 3-dimensional view is lost in transversal cuts. To avoid this problem, Taylor and Lee[29] simulated calculations in which the microcracks displayed themselves as ellipses possessing specific axial ratios (4.5:1) with a standardized ratio of 0:1.

In our investigation, some differences must be taken into consideration. The mechanism of the cracking is different. Microcracks formed from stress fractures lie within the bone, but microcracks caused by preparation were at the edge of the bone. The size and number of microcracks were subject to a much larger variance. The course of the microcracks in the 3-dimensional structure presented itself differently. No distinct alignment resulted. Whole chunks of mineralized tissue were loosened. The third dimension could be neglected because it corresponded to the length of the prepared bone. For these reasons, we limit our description to a defect zone. The zone created by the piezoelectric device (approximately 170 μm) was more than 3 times as deep as that of the rotary bur (approximately 54 μm) and showed a more invasive character, which could be an advantage for the healing process. The increased surface area might induce an activation of more osteoclasts and osteoblasts.[22,24] An exact differentiation between cancellous bone and cortex was not possible.

The usual definition in the literature of nerve lesions consists of morphological changes and the accompanying loss of function.[30,31] Lesions in our study refer only to histomorphological changes, which appear during preparation. Reaction of the dead nerve tissue accompanied with functional loss could not be examined. Histological lesions were limited to the epineurium in the group treated with the piezoelectric device.

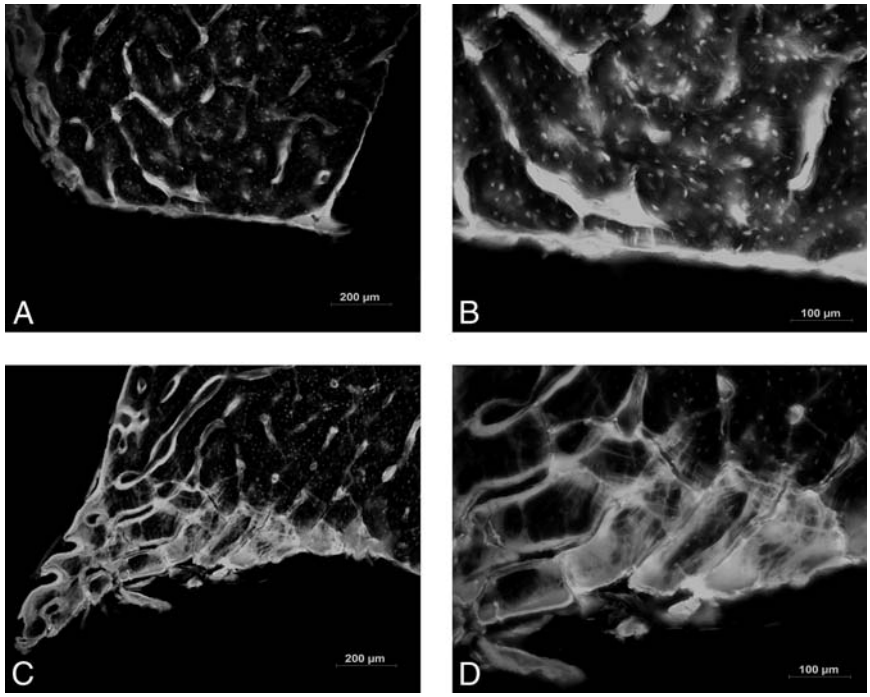

FIGURE 4. Histological photomicrographs of the prepared alveolar bone edge stained en bloc with basic fuchsin. Stained areas appear orange under green epifluorescence (magnifications ×100 and ×200). (A, B) Bone edge prepared with the rotary bur. Smooth cut bone surface with few isolated cracks. (C, D) Bone edge prepared with the piezoelectric device. Irregular cut bone surface with loosened hard substance.

TABLE 3
Measurement values of the defect zones (μm)

	Rotary Bur	Piezoelectric Device
Mean ± SD	53.51 ± 18.59	169.69 ± 49.63
Minimum	24.28	114.58
Maximum	92.88	258.35

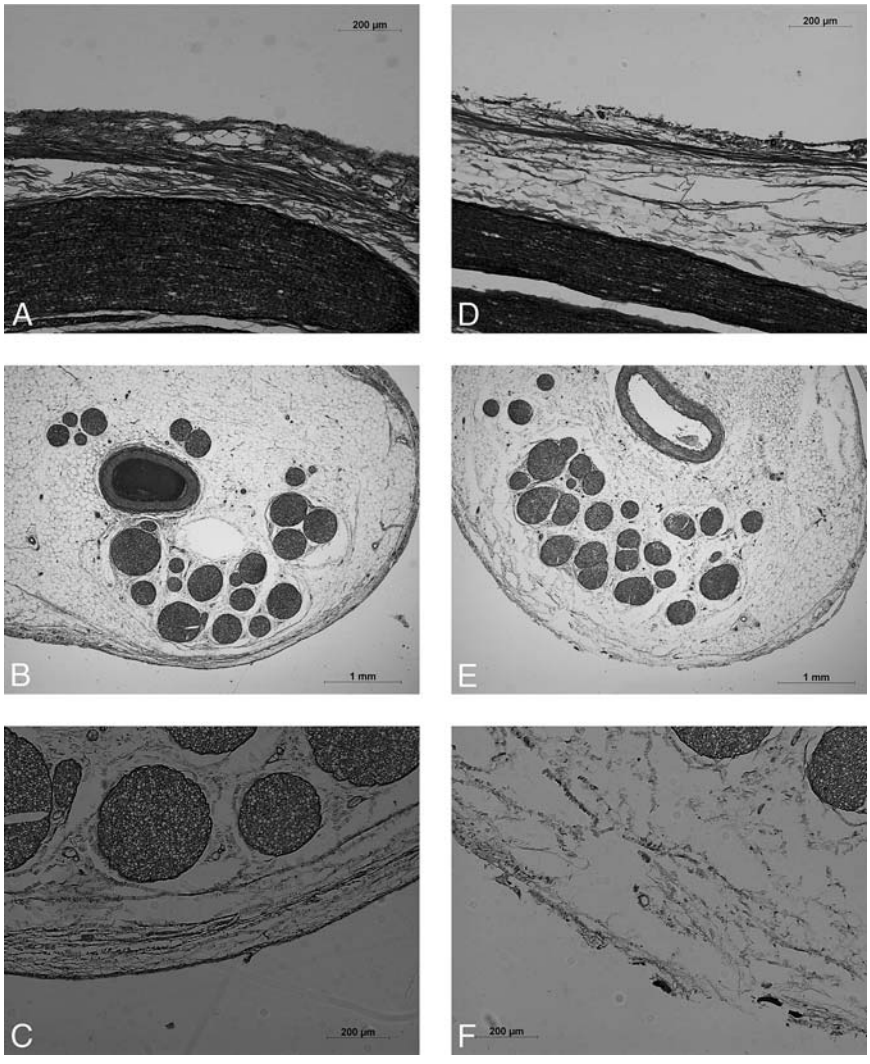

FIGURE 5. Histological photomicrographs of the inferior alveolar nerve (IAN) sections. Nerve touched by the thin bent spatula during preparation with the rotary bur. (A) IAN cut lengthwise to the fascicles in the posterior part (magnification ×100). (B) IAN cut crosswise to the fascicles in the anterior part (magnification ×25). (C) IAN cut crosswise to the fascicles in the anterior part (magnification ×100). Nerve touched by the insertion of the piezoelectric device. (D) IAN cut lengthwise to the fascicles in the posterior part (magnification ×100). (E) IAN cut crosswise to the fascicles in the anterior part (magnification ×25). (F) IAN cut crosswise to the fascicles in the anterior part (magnification ×100).

The advantage of the ultrasonic instruments is a claimed inactive effect on soft tissue.[10] The explanation for this phenomenon is that soft tissue gives way to the instrument's oscillation and thus does not represent a target. The lesions in the epineurium shown in this study can be explained by the roughness of the insert in addition to the relative rigidity of the epineurium. If the tissue has a high rigidity, the moment of inertia is too large to follow the oscillations, and lower-rigidity tissue injuries at the surface will result. Because injuries could be observed only at the surface of the epineurium, a decreased oscillation seems to be linked with increased depth (Figure 6).

The function of the epineurium is to protect the nerve fibers. It contains important cellular components and vessels required for repair mechanisms. However, these fibers are more vulnerable than those of the endoneurium.[31,32] A lesion of the epineurium is accompanied by a morphological change. Extraneural scar formation as a consequence of the healing process can compress or rotate the peripheral nerves, and fibrous ankylosis can lead to restriction of the slip motion.

The operational interference after conventional transposition or transposition with a bur frequently causes a well-known sensitivity disturbance of the area served by the IAN. This is probably because of the mobilization and the associated stretching of the nerve, which can be stretched about 10% to 20% before structural changes develop.[33] With increasing tension, the nerve moves within its canal and uses the range of the loose flexible fibers. Tearing of the axons occurs only when they are overstretched.[30] The prognosis of these lesions after conventional lateralization or transposition of the IAN is reported to be very good (healing between 80% and 100%[1,2]). Initial healing is observed after 3.8 to 5.7 weeks and complete recovery after 6 months to 1 year.[1,5–7] These statements refer to a lateralization without complications.

Further investigation should aim to reveal the damage to the nerve during preparation with the piezoelectric device. This could be done on the basis of in vivo studies with the help of somatosensory-evoked potentials for the objective measurement of nerve damage. If the marginal injuries to the epineurium prove to be tolerable, lateralization with the piezoelectric device might be regarded as a safe and easy method.

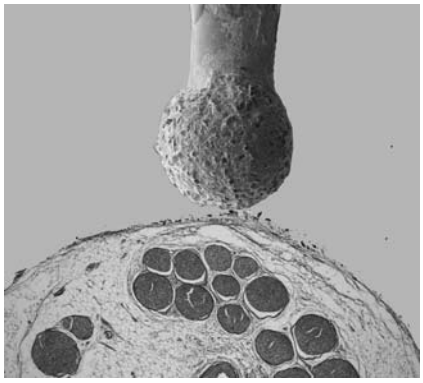

FIGURE 6. The moment the piezoelectric insert touches the nerve. Proportions were retained (enlargement ×25).

CONCLUSIONS

In vitro preparation with the piezoelectric device was more invasive to the bone than with the conventional diamond bur. In fact, touching the IAN resulted in roughening of the epineurium, but deeper structures remained unaffected. Therefore, within the parameters of this in vitro study, the degree and risk of injury with the piezoelectric device was lower than with the conventional rotary bur.

REFERENCES

1. Nocini PF, De Santis D, Fracasso E, Zanette G. Clinical and electrophysiological assessment of inferior alveolar nerve function after lateral nerve transposition. *Clin Oral Implants Res.* 1999;10:120–130.

2. Sandstedt P, Sörensen S. Neurosensory disturbances of the trigeminal nerve: a long-term follow-up of traumatic injuries. *J Oral Maxillofac Surg.* 1995; 53:498–505.

3. Hausamen JE, Schmelzeisen R. Current principles in microsurgical nerve repair. *Br J Oral Maxillofac Surg.* 1996; 34:143–157.

4. Peleg M, Mazor Z, Chaushu G, Garg AK. Lateralization of the inferior alveolar nerve with simultaneous implant placement: a modified technique. *Int J Oral Maxillofac Implants.* 2002;17:101–106.

5. Rosenquist B. Fixture placement posterior to the mental foramen with transpositioning of the inferior alveolar nerve. *Int J Oral Maxillofac Implants.* 1992; 7:45–50.

6. Hirsch JM, Branemark PI. Fixture stability and nerve function after transposition and lateralization of the inferior alveolar nerve and fixture installation. *Br J Oral Maxillofac Surg.* 1995;33:276–281.

7. Morrison A, Chiarot M, Kirby S. Mental nerve function after inferior alveolar nerve transposition for placement of dental implants. *J Can Dent Assoc.* 2002; 68:46–50.

8. Vercellotti T, De Paoli S, Nevins M. The piezoelectric bony window osteotomy and sinus membrane elevation: introduction of a new technique for simplification of the sinus augmentation procedure. *Int J Periodont Restor Dent.* 2001;21:561–567.

9. Brent PD, Morgan LA, Marshall JG, Baumgartner JC. Evaluation of diamond-coated ultrasonic instruments for root-end preparation. *J Endod.* 1999;25: 672–675.

10. Torrella F, Pitarch J, Cabanes G, Anitua E. Ultrasonic ostectomy for the surgical approach of the maxillary sinus: a technical note. *Int J Oral Maxillofac Implants.* 1998;13:697–700.

11. Vercellotti T. Piezoelectric surgery in implantology: a case report—a new piezoelectric ridge expansion technique. *Int J Periodont Restor Dent.* 2000;20:358–365.

12. Vercellotti T, Russo C, Gianotti S. A new piezoelectric ridge expansion technique in the lower arch—a case report. *World Dent 2000.* 2003;2:1–3.

13. Howaldt H-P, Schmelzeisen R. *Neuropathien und Nervenrekonstruktion.* München, Jena, Germany: Urban & Fischer; 2002.

14. Winand O. REM-Studie zur Ablationsqualität der piezoelektronischen Knochenchirurgie. *ZMK.* 2003;19:562–566.

15. Globtek Implant Systems, Brazil. Han D-H, Jeon Y-S, Kim J, Kim S-J. A comparative study of two threaded CP titanium implants. Part I: surface analysis and histologic evaluation of bone healing. Available at: http://www.globtek.com.br/profissionais/research/surface_analysis.pdf. Accessed December 27, 2005.

16. Burr DB, Hooser M. Alterations to the en bloc basic fuchsin staining protocol for the demonstration of microdamage produced in vivo. *Bone.* 1995;17: 431–433.

17. Huja SS, Hasan MS, Pidaparti R, et al. Development of a fluorescent light technique for evaluating microdamage in bone subjected to fatigue loading. *J Biomech.* 1999;32:1243–1249.

18. Lee TC, Myers ER, Hayes WC. Fluorescence-aided detection of microdamage in compact bone. *J Anat.* 1998; 193 (pt 2):179–184.

19. Murphy TR, Thomson JM. The number and size of myelinated fibres in the inferior alveolar nerve of a young sheep. *Arch Oral Biol.* 1966;11:307–314.

20. Bucher O, Wartenberg H. *Peripheres Nervensystem.* Bern, Switzerland: Hans Huber Verlag; 1997.

21. Haribhakti VV. The dentate adult human mandible: an anatomic basis for surgical decision making. *Plast Reconstr Surg.* 1996;97:536–541, discussion 542–543.

22. Khambay BS, Walmsley AD. Investigations into the use of an ultrasonic chisel to cut bone. Part 1: forces applied by clinicians. *J Dent.* 2000;28:31–37.

23. Mazorow HB. Bone repair after experimentally produced defects. *J Oral Surg Anesthetol Hosp Dent Serv.* 1960;18: 107–115.

24. Khambay BS, Walmsley AD. Investigations into the use of an ultrasonic chisel to cut bone. Part 2: cutting ability. *J Dent.* 2000;28:39–44.

25. Horton JE, Tarpley TM Jr, Wood LD. The healing of surgical defects in alveolar bone produced with ultrasonic instrumentation, chisel, and rotary bur. *Oral Surg Oral Med Oral Pathol Oral Radiol Endod.* 1975;39:536–546.

26. Horton JE, Tarpley TM Jr, Jacoway JR. Clinical applications of ultrasonic instrumentation in the surgical removal of bone. *Oral Surg Oral Med Oral Pathol Oral Radiol Endod.* 1981;51:236–242.

27. McFall TA, Yamane GM, Burnett GW. Comparison of the cutting effect on bone of an ultrasonic cutting device and burs. *J Oral Surg Anesthetol Hosp Dent Serv.* 1961;1:200–209.

28. Burr DB, Stafford T. Validity of the bulk-staining technique to separate artifactual from in vivo bone microdamage. *Clin Orthop.* 1990;260:305–308.

29. Taylor D, Lee TC. Measuring the shape and size of microcracks in bone. *J Biomech.* 1998;31:1177–1180.

30. Davison SP, McCaffrey TV, Porter MN, Manders E. Improved nerve regeneration with neutralization of transforming growth factor-beta1. *Laryngoscope.* 1999;109:631–635.

31. Grant GA, Goodkin R, Kliot M. Evaluation and surgical management of peripheral nerve problems. *Neurosurgery.* 1999;44:825–839, discussion 839–840.

32. Rempel D, Dahlin LB, Lundborg G. Pathophysiology of nerve compression syndromes: response of peripheral nerves to loading. *J Bone Joint Surg Am.* 1999;11:1600–1610.

33. Gellrich NC, Schramm A, Rustemeyer J, Schon R, Theodor Eysel U. Quantification of the neurodegenerative impact on visual system following sudden retrobulbar expanding lesions—an experimental model. *J Craniomaxillofac Surg.* 2002;30:230–236.